Piezoelectric Springs for Novel Geophone Sensors

David Pearce and James Holmes, Functional Materials Group, Interdisciplinary Research Centre (IRC) in Materials for High Performance Applications, The University of Birmingham, Edgbaston, Birmingham B15 2TT, UK. Tel: 0121-414-7122/7836, Fax: 0121-414-3441, email: d.h.pearce@bham.ac.uk, Web: http://fmg.bham.ac.uk/

A. Summary of Work

A.1. Abstract

Helically coiled ceramic piezoelectric springs have recently been developed at the University of Birmingham for use as potential vibration sensors. The purpose of this programme of work was to investigate in more detail than had been possible previously, the behaviour of such devices, in terms of their response to vibrations in the range of frequencies commonly used in geophysical applications, i.e. from ten to several hundred Hertz. As part of this programme, a vibration analysis apparatus was set up, to determine accurately the frequency response of various piezoelectric springs. Results have been obtained which illustrate the main features of the behaviour of these springs. In brief, the typical electrical output behaviour of a light multi-turn spring with a small seismic mass is described by a strong fundamental longitudinal resonance, followed at higher frequencies by many separate overtones, resulting in a very crowded frequency spectrum. This type of output is undesirable for seismic applications, where more flat frequency responses are required. However, by altering the design of the spring-mass system the undesired overtones can be moved up the frequency spectrum away from the measurement area. This design approach may be useful in developing a suitable piezoelectric geophone to compete with conventional electromagnetic types.

A.2. Introduction

Piezoelectric materials are commonly used in sensing and transmitting applications associated with acoustic waves, particularly in underwater applications. Examples of these are hydrophones, where the sensitivity of the material to pressure changes is important, and in sonar projectors, where the efficiency of converting electrical to acoustic energy in the material is utilised. In the bulk form, ceramic piezoelectrics such as lead zirconate titanate (PZT) are sensitive to small changes in the stress state within the material, and to a first approximation a linear response of electrical signal to stress can be obtained. This results in very low distortion and low noise devices. The nature of the material, however, means that in its bulk form the signals which can be obtained from solid blocks subjected to small vibrations are very small. Piezoelectric vibration sensing devices therefore are commonly interfaced with equipment through a charge amplifier. The small signal, together with the need to use amplification, with the necessary shielding to minimise noise, has prevented PZT devices from being widely used in geophysical applications, where very small seismic vibrations need to be detected. Current technology for seismic sensing generally utilises more conventional moving coil (or possibly moving magnet) devices, which generate signals electromagnetically. The resolution of these devices is limited by the noise and distortion to which they are susceptible, while the size and mass of the device are restricted by the need to use strong magnets and tightly wound wire coils. A combination of the high signal output at low frequencies possible through such conventional geophones, with the low noise and distortion of a piezoelectric device, would result in a much improved device. A possible solution to this has been found, through the application of coiled tubular PZT structures. By forming the PZT into a coil, the effective stiffness of the axial direction is reduced dramatically, resulting in the possibility of a much improved response at low frequencies.

A.3. Experimental Method

The basic form of the springs that were fabricated for this project is shown in Figure 1. The springs were formed through extrusion of a plastisized ceramic powder dispersion or dough through a tubular die, followed by winding of the extrudate around suitably sized formers. These springs were sintered, electroded and poled, with the electrode faces being on the inner and outer faces of the tube section and the poling direction through the wall thickness. Mounting of the devices was achieved by bonding to a suitable base and a top seismic mass (if used). The vibrational behaviour of the devices was characterised by attaching the base to a vibrating plate. The amplitude and frequency of the vibration signal fed to the device was controlled by computer, and the signal obtained from the device compared with the input, fed to the same computer. A calibrated piezoelectric accelerometer was used to obtain a reference point for the acceleration at the base, from which the velocity and displacement sensitivities could be determined.

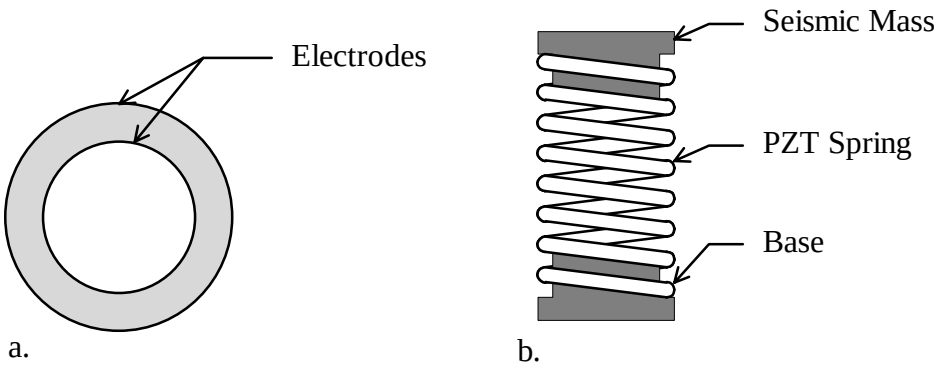

Figure 1 – Basic form of the tubular helical piezoelectric spring, showing a) the electrode connections, and b) the sensor assembly.

A.4. Results

Measurements of voltage output and resonant frequency with applied seismic mass were taken on various springs. The relationship between seismic mass and resonant frequency was found to be close to that expected, and predicted the contribution of the spring self mass to the seismic mass correctly. The main feature of the vibration response of piezoelectric springs over a wide frequency range is large number of resonances. This has been explained through consideration of the different modes of resonance which are predicted to appear, and the higher frequency harmonics of these. For multiple turn springs with a low seismic mass compared with the spring mass, a typical response obtained is shown in Figure 2a. This illustrates the main problem to be overcome when designing piezo spring seismic sensors. By using a much larger seismic mass, and a spring with only a small number of turns, a much flatter frequency response can be obtained, shown in Figure 2b. This result points the way to designing a suitable seismic sensor for the required frequency range in the field.

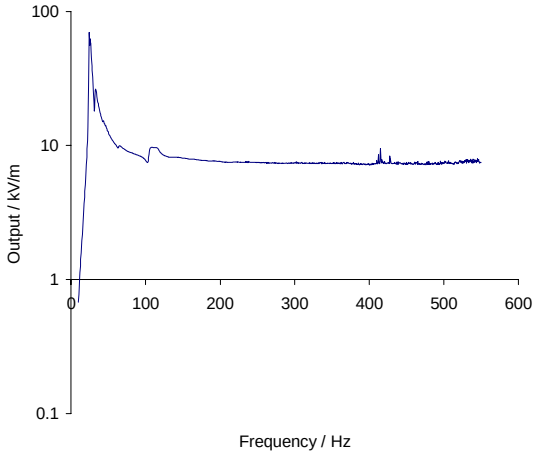

a. b.

Figure 2 - Frequency responses of a). a multi turn piezo spring with no seismic mass; b). a short piezo spring with a large seismic mass.

A.5. Conclusions and further work

Through many measured observations of the voltage output and frequency response of various geometries of piezoelectric springs, the main features of such devices have been recorded and understood. The results obtained present a picture of how these springs behave in real vibration situations, and have uncovered many features of their operation. Piezoelectric springs behave in a completely different way to conventional geophones, and as such require different design rules.

The IRC now has a sophisticated and flexible system for measuring the response of devices to vibrations, and this will be useful in furthering this work to develop improved devices. Future work is planned on obtaining flatter frequency responses through the use of low stiffness springs of low mass, combined with relatively high seismic masses, while keeping the whole device as light as possible. The challenge to design a workable piezoelectric geophone is still great, but the results to date have shown promise for this approach.

B. Technical Report

B.1. Background to the Work Programme

This research arises out of efforts to improve ceramic processing technology undertaken by the ICI Solid State Science Group in the 1980s, when the technique of Viscous Processing (VP) was developed. This is a ceramic processing technique whereby a highly dispersed ceramic powder and soluble polymer medium paste is generated through the application of very high shear stresses. These stiff pastes can be formed into shapes through numerous conventional plastics forming techniques such as calendering, pressing, die-stamping, press forming and extrusion. An often-used example of the uniformity and high strength of ceramic materials produced through VP has been a ceramic spring, an example which has yet to provide a useful application. This type of structure illustrates well the key benefits of VP, since when a spring undergoes extension or compression the material from which it is formed experiences a high stress uniformly distributed over the length of the spring. Ceramics are brittle materials and hence the point of failure is always determined by the position of the largest flaw in the stressed part of a component. Since VP very effectively reduces the size of these flaws in the final sintered material, through breakdown of agglomerates in the green state, the stress at which a component will fail can often be greatly increased. Alternatively, the volume fraction of material under a normal stress can be increased, allowing the generation of previously impractical device geometries such as springs.

After part of the ICI effort in ceramic processing (the Functional Materials Group) was transferred to the University of Birmingham, work began on applying VP to piezoelectric materials, notably Lead Zirconate Titanate (PZT), the most commonly used piezoelectric ceramic. In this electrically functional material, the concept of a spring becomes one which can have potentially numerous device applications, through the coupling of mechanical movement with electrical energy, both in the generation and detection of millimetre scale movements. Through discussions with underwater acoustics companies, ideas based on the use of a wound tubular device were put forward as possible flexible hydrophones. These devices were envisaged to operate in the conventional manner, i.e. by detecting changes in hydrostatic pressure in the surrounding fluid through hoop stresses set up in the wall of the piezoelectric tube. Since the device was designed to be of the simplest form possible, with blanket electrodes on the outer and inner surfaces of the tube, it was thought that movements in the axial direction of the spring and in various other bending and twisting configurations, would generate no net signal. This is because conventional piezoelectric theory requires a net strain to be applied in the poling direction to generate an electrical signal. The two main stresses in a spring, torsion and bending would not generate any net strain in this direction. Thus the device would be highly sensitive to hydrostatic pressure changes whilst remaining resistant to high static pressures and resilient and unresponsive to macro-scale movements in the flexible hose into which the device would be mounted. However, once some initial test devices were fabricated it was soon discovered that such devices were indeed very responsive to large-scale deformations. Thought then turned to the application of such an unexpected result, and the most obvious one was seen to be the seismic geophone.

B.2. Conventional vs. Piezoelectric Geophones

Shown in Figure 3 is the basic form of a conventional moving coil geophone. The main component, though the simplest, is the central magnet, which provides the stationary field through which the wound wire coil passes. The electrical signal is generated from the coil moving relative to the magnet, which is part of the assembly attached firmly to the vibration source. The signal generated is out of phase with the movement of the base, and is directly proportional to the relative velocity of the coil and magnet. The frequency of resonance of such a device is determined by the combination of spring stiffness and overall coil and coil former mass. Damping of the device is achieved through design of the spring and through selection of a shunt resistor across the coil.

Comparing the conventional geophone with the proposed piezoelectric geophone shown in Figure 1, the differences are clear. In the piezoelectric geophone the coil and spring are in the same part, together with a portion of the mass. There is no magnet, and the signal is generated from the deflection of the seismic mass at the top of the spring relative to the base. Both devices operate out of phase with the base vibration above their fundamental resonance, though the piezoelectric device is displacement rather than velocity sensitive.

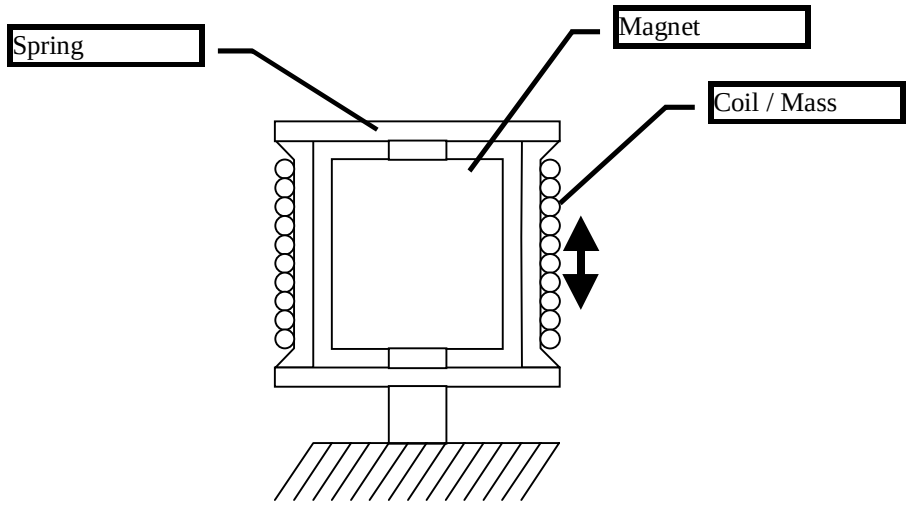

Figure 3 – Basic configuration of an electromagnetic seismic geophone.

In the case of the conventional geophone, the different functional elements of the device can be designed and engineered separate to one another, i.e. the spring element can be designed to have the optimum compliance for the frequency range chosen. Indeed, it is this spring design which appears to be crucial in obtaining the desired frequency response. In the case of the piezoelectric spring device, however, the design is complicated by the fact that the spring compliance, seismic mass and electrical generator are all connected in one component. This makes the task of generating design rules more difficult. This is the starting point for the work in this short programme, its aim being to begin to understand what is important in the design of a functional piezoelectric geophone.

B.3. Experimental Procedure

B.3.1. The Piezoelectric Spring Fabrication Route

Shown in Figure 4 is a flow diagram of the process route used to fabricate the piezoelectric springs used in this programme. This is similar to a conventional route used in industry to manufacture many types of piezoelectric components, and varies only in the first three stages. Firstly, and most importantly to the generation of a suitable spring, is the Viscous Processing stage. In this case the shear was generated through the use of a twin roll mill, shown schematically in Figure 5. The difference in rotational velocities of the counter-rotating rolls generates high shear forces in the nip between them. This rapidly homogenises the polymer/ceramic mixture and breaks apart any agglomerates that exist in the as-received powder state. Once these agglomerates are broken down they are prevented from re-forming by the presence of the highly concentrated viscous polymer solution medium in which they are suspended. The de-agglomerated dough is then removed from the rolls in the form of a thin sheet, which for the subsequent extrusion process has to be rolled into a feedstock rod.

Figure 6 illustrates the simple process of formation of a tubular extrudate. A load is applied to the plunger, forcing the dough through an annulus die. Immediately after extruding, the extrudate is wound on to a mandrel, into which is machined a screw thread appropriate for the spring pitch being generated. The material is then dried in this state, and the plastic dough transforms into a tough green state, which is strong enough to withstand being handled, so the spring can be removed from the mandrel.

For burnout and sintering the spring is placed on an alumina ceramic rod, chosen to be the appropriate diameter such that after the ceramic has undergone the 15% linear shrinkage which occurs during sintering the spring will closely fit the rod. This allows a uniform diameter spring to be generated without slumping. Without such support the spring would collapse, since at the high temperature used for sintering the material is prone to a great deal of creep.

After sintering, electrodes can be applied to the inner and outer surfaces of the tube. This is done by forcing a suspension of fine silver powder and glass frit through the tube, which leaves behind a thin coating, typically 5 microns in thickness. The outer part is coated with the same mixture by spraying or dipping. These electrodes then have to be fired on to the ceramic to bond intimately to the surfaces, for which the glass frit is used. After this final firing stage the electrical contacts are made to the silver electrodes and the device is poled. An oil bath held at 120 to 130^{o}C is used for this, to maintain the ceramic at a constant temperature and to prevent arcing across electrodes. An electric field of 2.5 kV/mm across the wall thickness of the tube is applied for 10 minutes to pole the material radially. The device is then ready for testing.

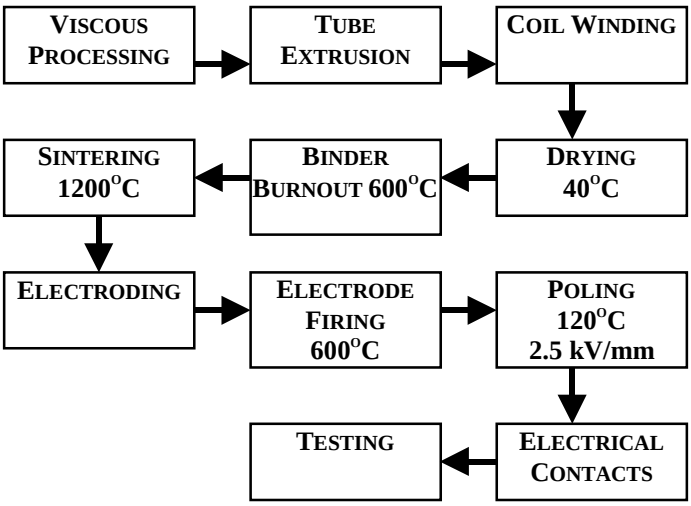

Figure 4 – Flow diagram of the piezoelectric spring fabrication route.

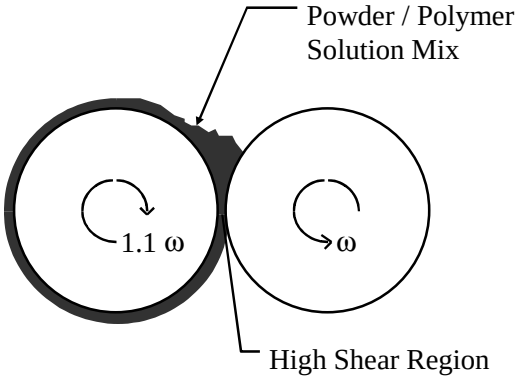

Figure 5 – Schematic diagram of twin roll milling process to generate a Viscous Processed ceramic dough.

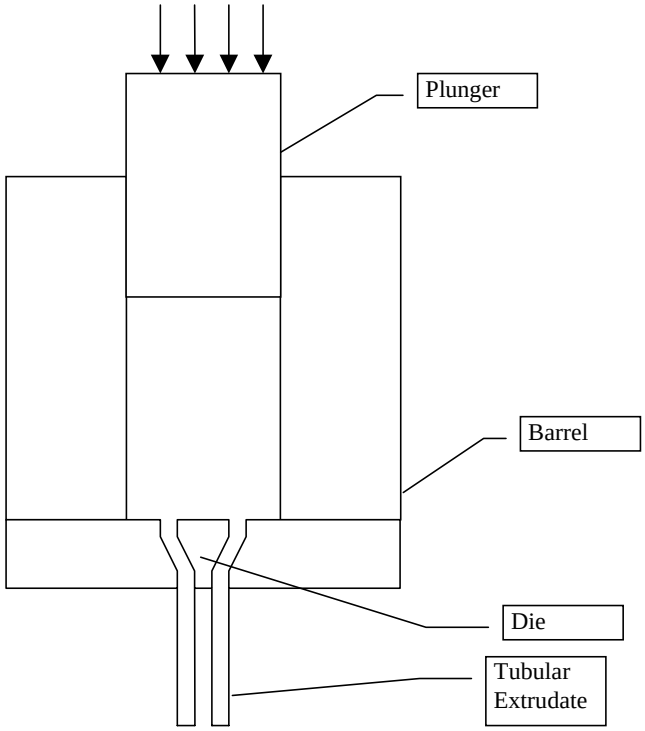

Figure 6 – Cross-section schematic of the tube extrusion process.

B.3.2. The Vibration Analysis Equipment

In order to begin the dynamic analysis of the springs it was necessary to spend time on setting up the vibration analysis equipment. The aims in the experimental set-up were to provide a versatile apparatus that could apply a sinusoidal drive of known amplitude to the device and measure the output from the device. It was also a necessity to have a longer term view to the potential needs of the testing equipment, as at the time the project commenced it was unknown what figures of merit were required or would prove useful.

A schematic of the final experimental set-up is illustrated in Figure 7, and the equipment purchased and employed for this is given in Table 1.

For the computer hardware requirements, input acquisition and output rates were not stringent due to the low frequency bandwidth of interest. However the accuracy of the measured signal was important in order to provide accurate measurements of distortion. Therefore it was decided to use an onboard multifunction input output card, with a maximum acquisition/update rate of 100 kSamples/s at 16-bit resolution. Signal conditioning was required due to the low-level of signal output from the springs. This was achieved using a SCXI_1767, which includes anti-aliasing filters.

The vibration source was required to provide sinusoidal displacements to a table without any resonances of its own within the measured frequency range. To this end a commercial electromagnetic shaker was employed. The power requirements were not stringent, so the low range vibration units were more than adequate. In this study the system specifications indicated a usable range in excess of 10 kHz and a suspension stiffness of 1.14 kg/mm which are both in excess of the requirements for a clear frequency spectrum. The current to the shaker was controlled by the output from the computer data-acquisition card, amplified by a linear amplifier.

To measure the amplitude of the vibration a commercial accelerometer/charge amplifier was used. The calibrated accelerometer was rated up to 4 kHz and 20 km/s^2 maximum acceleration. The signal from this unit was amplified by a charge amplifier which was in turn connected to the signal conditioning unit for input to the data acquisition card.

Initially it was intended to build a platform onto the shaker upon which the accelerometer and a number of devices were to be attached and tested. However the first platforms tested were found to have flexural resonances within the measurement range, so it was not possible to have confidence in these results. To be sure that the amplitude measured by the accelerometer was the same as that experienced by the test device the two were mounted vertically above one another. This was achieved by brazing a bottom plate attached to the shaker to a metal cylinder onto which a top plate was bolted. The devices on test were then attached by a screw thread to the top plate. This robust arrangement effectively removed all significant mechanical resonances well out of the measurement range.

A computer program written in LabView for Windows controlled the vibration amplitude using the output from the accelerometer/charge amplifier and adjusting the output appropriately. The user inputs the tolerances upon the vibration amplitude. Upon meeting the required tolerance the signal from the device on test is read from the signal-conditioning unit. A frequency sweep is performed between predetermined limits at defined intervals and the user specifies the amplitude in terms of a definition of displacement, velocity or acceleration levels that are maintained constant throughout the frequency sweep.

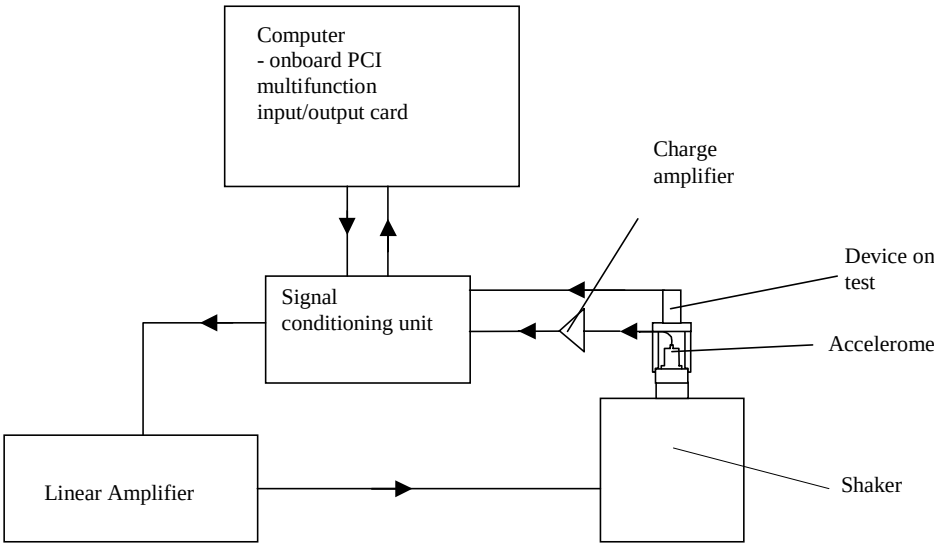

Figure 7 – Schematic diagram of the experimental set-up to analyse the spring vibration responses.

Table 1 – Experimental set-up components and sources.

Description	Part No.	Manufacturer
Accelerometer	Type 4370	Brüel & Kjær
Charge Amplifier	Type 2634	Brüel & Kjær
Shaker	V20	Gearing & Watson
Linear Amplifier	PA100	Gearing & Watson
Multifunction I/O Card	MIO-16	National Instruments
Signal Conditioning	SCXII - 1657	National Instruments

B.3.3. Original Experimental Aims

As mentioned in the original proposal, the experimental aims were basically to fabricate and characterise a range of springs of varying geometries. This data would then be used as the basis for future design of geophone sensors. It was proposed to fabricate springs of tubular cross-sections varying from 1 to 3 mm, and formed into springs of diameters ranging from 10 to 30 mm. Varying the applied seismic masses would then allow the simple relationship between the resonant frequency of a mass-spring system to be confirmed:

$$\omega = \sqrt{\frac{k}{m}} \qquad \textbf{Equation 1}$$

where ω is the resonant frequency in rad/s, k the spring constant in N/m and m the seismic mass in g.
Measurements were to be taken over the frequency range of interest using the aforementioned equipment, covering frequency response, output linearity and signal to noise ratio. To some extent these simple aims have been covered in the work programme, but as is illustrated in the following section some of the aims have been altered due to the nature of the results obtained.
The original work programme timetable is shown in Table 2. This is largely how the experimental work proceeded, though with the work in months 3 and 4 extended by approximately 6 weeks, due to difficulties in spring fabrication and problems associated with faulty pieces of equipment necessitating return to the manufacturer.

Table 2 – Original work programme timetable

	Month					
Task	**1**	**2**	**3**	**4**	**5**	**6**
Die Design and Fabrication	■					
Testing Apparatus Construction	■	■				
Spring Fabrication		■	■	■		
Electromechanical Testing			■	■	■	■
Final Report						■

B.4. Results

B.4.1. Single frequency responses

B.4.1.1. Variation in resonant frequency with applied seismic mass

The results shown in this section are for springs with several turns and seismic masses which are less than or of a similar mass to that of the spring itself. The importance of this will be made clear later on. For this type of device, the typical variation in the fundamental resonant frequency is shown in Figure 8, which shows the direct relationship between the resonant frequency and the applied seismic mass, i.e. not taking into account the self mass of the spring. Figure 8b shows the same data plotted such that the inverse square of the resonant frequency is shown versus the seismic mass. The straight line fitted to this relationship indicates that the basic equation (Equation 1) holds for this system. This also indicates that the effective mass contributed by the spring is 7.5g, 0.4 of the total spring mass. This compares very well with the expected calculated result (see Appendix A). The gradient of the curve in Figure 8b indicates a spring constant of 330 N/m, compared with a calculated constant of 600 N/m. This discrepancy obviously indicates that the spring behaviour is still poorly understood at this stage. The factors contributing to this result, compared to that calculated using ideal material constants and geometries are several. Firstly, the dimensions and the geometry of the springs fabricated for this project were not ideal. Due to the fabrication process, the circular extruded cross-section was prone to ovalisation during drying. The control over the pitch angle was not perfect, arising from creep during sintering causing slanting of the spring turns. Finally, and most crucially, the material constants used for modelling would not necessarily be the same in the final sintered and poled device, due mainly to the anisotropic nature of piezoelectric materials. This makes

applying mechanical models to piezoelectric structures an over-simplification. Modelling work currently underway at the University of Birmingham should be able to address these problems in future.

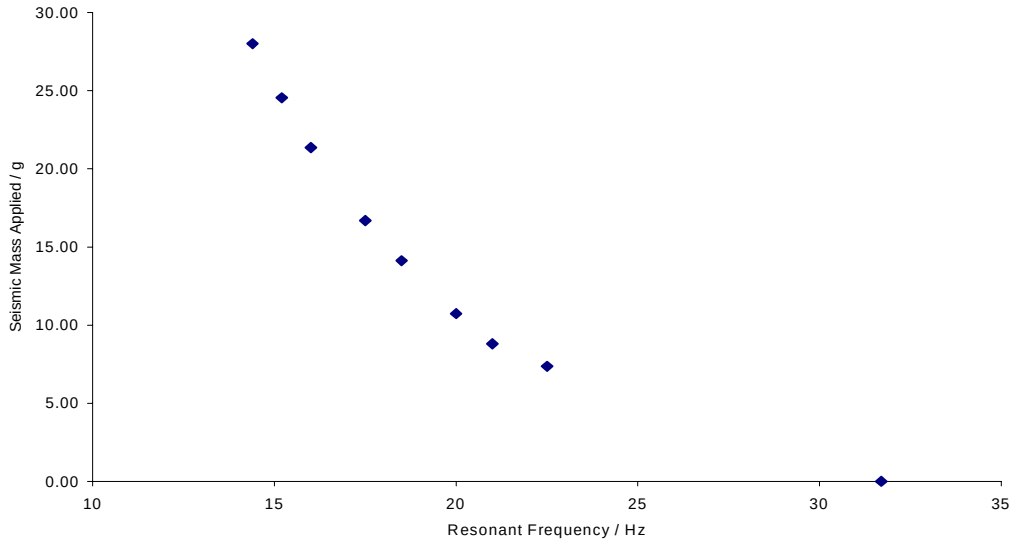

a.

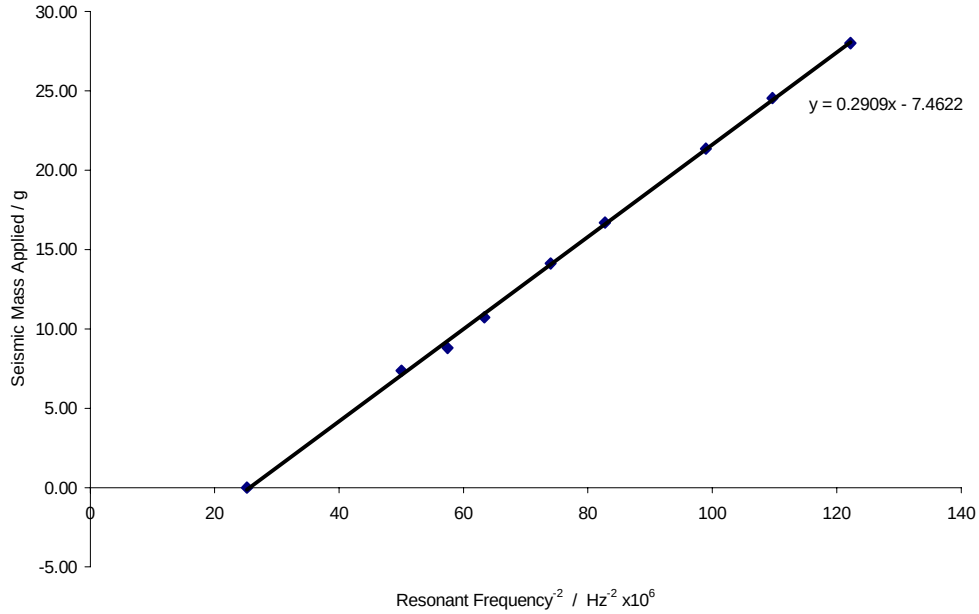

b.

Figure 8 – Variation in fundamental resonant frequency with applied seismic mass: a. mass versus frequency; b. mass versus inverse square root of frequency.

B.4.1.2. Variation in output amplitude with applied seismic mass

An as-yet unexplained result was obtained when measuring the effect of the seismic mass on the voltage output of the same type of spring. Taking the voltage output away from resonance (at 100 Hz), the variation is shown in Figure 9. This illustrates a significant increase in voltage output with applied mass. This result was also qualitatively observed in reverse. When applying a high voltage signal to a spring, a mechanical pre-load would increase the apparent force the spring was able to apply. It appears, therefore, that the effect of the mass in increasing the voltage output is through the pre-compression applied to the spring rather than simply the effect of an increased mass, i.e. inertia, restricting the movement of the top of the spring relative to the base.

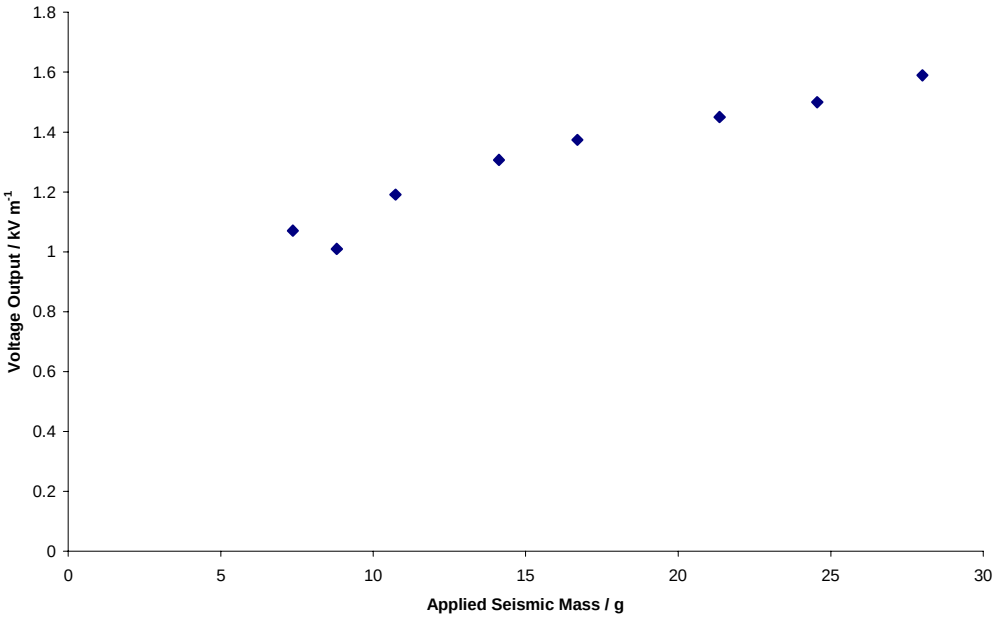

Figure 9 – Variation in voltage output versus applied seismic mass for a multi-turn spring.

B.4.2. Full frequency range response results

The first and most obvious result to obtain from the newly set up vibrational analysis equipment was the response of a multi-turn spring without a seismic mass. The result of this analysis is shown in Figure 10. A very complicated frequency response is evident, with the fundamental longitudinal resonance the most prominent. Calculations of the fundamental resonances predicted values of 57.3 Hz for the compressive mode and 50.7 Hz for the flexural mode. Since the spring was of a close-coiled type the compressive mode would be the more prominent, as the stresses involved are in torsion, while the flexural mode stresses are in bending. From simple spring analysis it can be shown that the stresses in torsion vary in proportion to the cosine of the pitch angle, while the bending stresses vary with the sine of the angle. At low angles therefore the torsional stresses are much greater. This prediction is confirmed by the two resonances at 48.9 Hz and 56.2 Hz in Figure 10, likely to be the flexural and torsional resonances respectively. The predicted frequencies, as well as the relative amplitudes, are in line with those measured. As for the rest of the frequency response, the results become increasingly difficult to interpret. The low frequency resonance, at 33.4 Hz, is likely to be a shearing mode, generated by imperfect alignment of the spring to the vertical axis of vibration. Above the fundamental resonances are many separate and overlapping harmonics, though the resonances at 149 and 168 Hz can be confidently attributed to 3x multiples of the flexural and torsional fundamentals. The more complex picture above these frequencies arises from the many modes which a spring possessing a significant self mass appears to be able to generate.

Varying the d_o/D ratio (outer diameter of the coil tube to the spring diameter), the predictions for the fundamental resonances hold, and the frequency spectrum remains just as crowded. Shown in Figure 11 are the results for a spring of similar tube diameter but of a smaller spring diameter. For this spring, the predicted torsional and flexural resonances were at 32.5 and 28.7 Hz, compared to the measured results of 35.8 and 30 Hz. In this case the flexural mode is more prominent relative to the torsional mode, due to the changed geometry of the spring and probable variations in tube cross-section causing preference for one mode over another. This is evidenced further by the results obtained for a spring with a smaller d_o/d_i ratio, i.e. one with a thinner tube wall. This type of tube extrusion is more prone to deformation during drying, caused by shrinkage of the spring diameter on to the spring former and resulting in an ovalisation of the cross-section. The frequency response of such a spring is shown in Figure 12. In this, the predicted torsional and flexural resonances are still close to those observed, 96.3 and 84.9 Hz, compared with 90.7 and 103 Hz respectively. The higher harmonics, however, depart from those previously observed, in that the peak at 409 Hz does not follow as a multiple of the fundamental resonances. In addition, the torsional harmonics do not appear to be as prominent as those associated with the flexural modes.

From these initial results it appears clear that piezoelectric springs in their fundamental form, while sensitive to vibrations over the required frequency range, do not give the required type of frequency response, due to the appearance of many overtones of the fundamental resonances. Understanding the modes which are likely to appear when vibrating a piezoelectric spring does, however, enable the designer to arrive at possible solutions, which are outlined in the following sections.

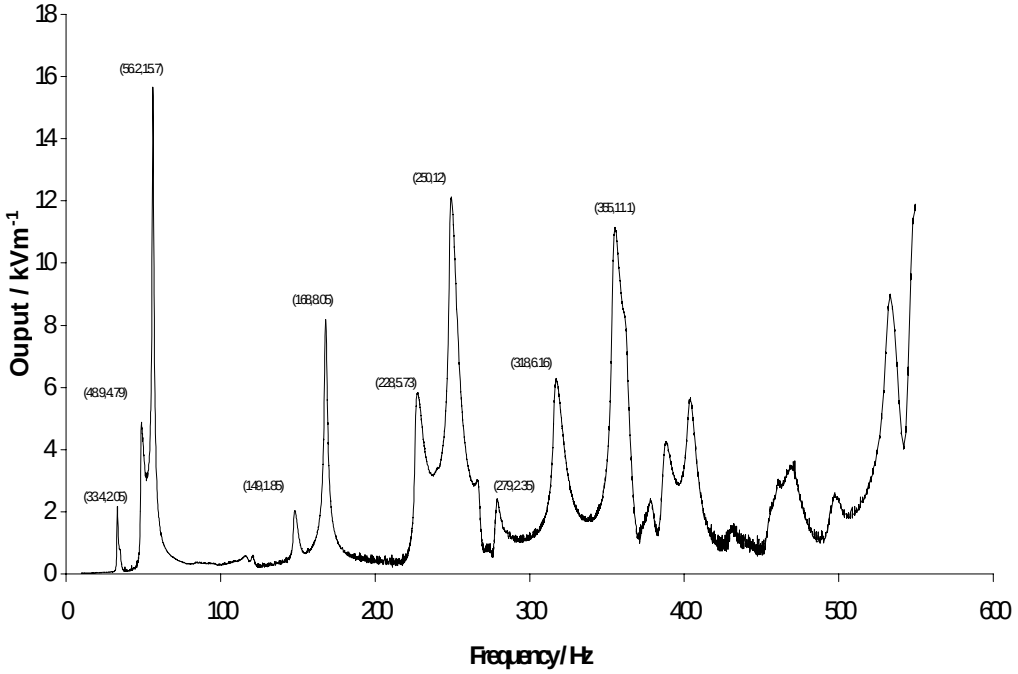

Figure 10 – Frequency response for a multi-turn spring without applied seismic mass (d_o=1.6 mm, D=21.6mm).

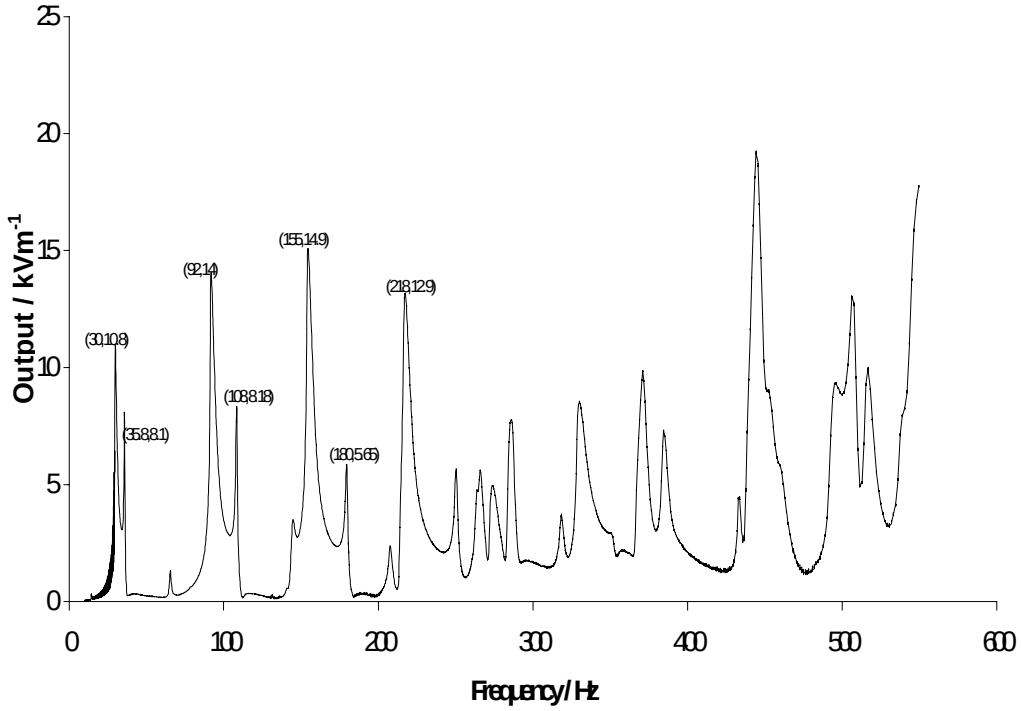

Figure 11 - Frequency response for a multi-turn spring without applied seismic mass (d_o=1.6 mm, D=16mm).

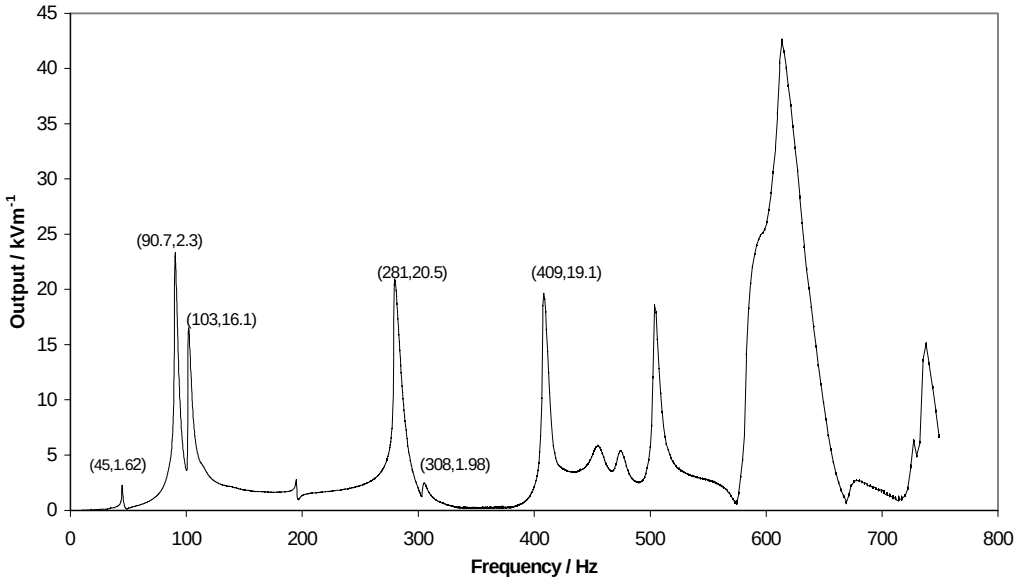

Figure 12 - Frequency response for a thin walled multi-turn spring without applied seismic mass (d_o=2.66mm, d_i=1.7mm, D=18.7mm).

B.4.3. The effect of seismic mass on the frequency response of a piezo spring

The question of how the higher resonances are affected by the application of a seismic mass is now addressed. Applying different masses to the spring and taking a frequency spectrum over a range where the first harmonics occur, the position and relative magnitude to that at 100 Hz of the first harmonics were noted. Figure 13 shows the frequency spectrum for a spring with two different seismic masses applied. The main feature of this is that the output at 100 Hz away from resonance increases with applied mass, and this applies over a wider frequency range. The occurrence of the peak at 160 Hz is due to coupling to a higher mode at 320 Hz. This frequency doubling may be observed on the output signal from the spring. The mass of the spring used was 4.6 g, so even increasing the seismic mass to over six times that of the spring has not reduced the strength of the resonance significantly. It was unclear if the strength of the resonance was due to the movement of the seismic mass or inhomegeneity of the spring. The spring was therefore clamped at the top by a mounting plate connected to the base of the shaker. The frequency spectrum for this arrangement, in the region of the major resonance, is shown in Figure 14. The resonance at 160 Hz is still prominent, suggesting that inhomegeneity over the length of the spring is responsible for the output.

It seems that in order to produce a clear frequency spectrum, the spring geometry must be such that no resonances occur within the frequency band of interest. This creates a fundamental problem in that in order to produce a high natural frequency the structure must be stiff with a low self-mass. Having a large spring constant also means that the seismic mass must be large. In such a situation the majority of the mass in the device will be comprised of the seismic mass, and not active material. The charge produced will therefore be relatively low.

In order to show whether such a situation is at all possible, it was decided to construct a spring from a tube with thin wall section (0.5 mm) but relatively large inner diameter (1.7 mm). The major spring dimensions were chosen to make the natural frequency of the unclamped spring high, a major diameter of 16 mm and consisting of only three turns. Such a construction will provide a high spring constant with low self mass and possess the strength to withstand a high seismic mass. This design is predicted to give the first natural frequency at 480 Hz, and if the ends were clamped a resonance of about 1000 Hz. A seismic mass of 270g was then applied, and the resulting frequency spectrum taken, shown in Figure 15. This shows a relatively flat output with displacement, slightly noisy at the higher frequencies. There is no observable coupling at 500 Hz with the longitudinal mode at 1000 Hz. The results were taken at a constant velocity vibration of 5 x 10^{-3} ms^{-1}, therefore at 500 Hz the device was measuring a displacement of 1.6μm, producing an output of 11.8 mV. The noise is therefore more prominent at the higher frequencies. Comparing this response to that of a conventional geophone, shown in Figure 16, it is clear that this approach indicates a potential way forward for utilising piezo springs as vibration sensors. One important point to be noted, however, is that the results for the piezoelectric spring are given in terms of displacement, whereas the geophone results are given in terms of velocity. This is due to the fundamental differences in operation of piezoelectrics, being displacement sensitive, compared to electromagnet sensors, being velocity sensitive.

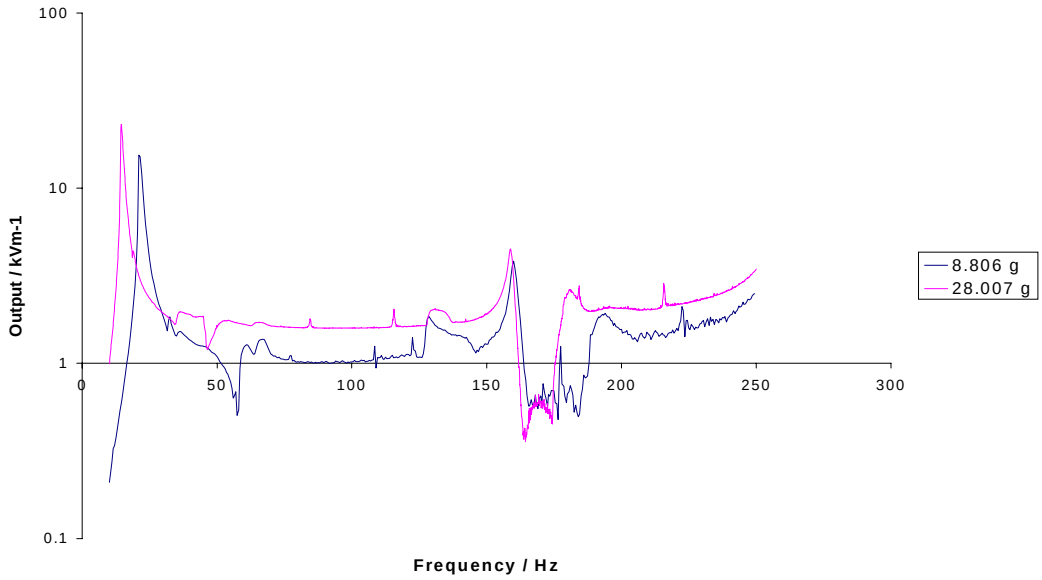

Figure 13 – The effect of seismic mass variations on the frequency spectrum of a piezo spring.

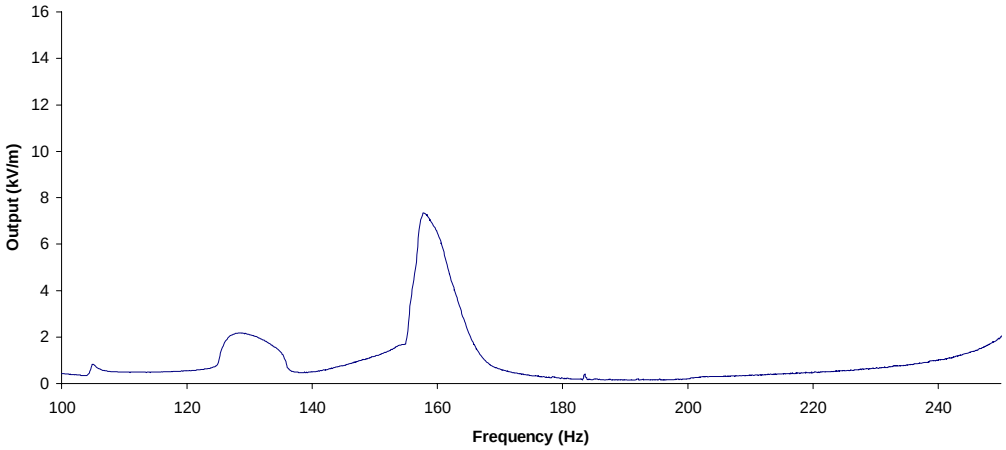

Figure 14 – Frequency response of a piezo spring with the top clamped in relation to the base.

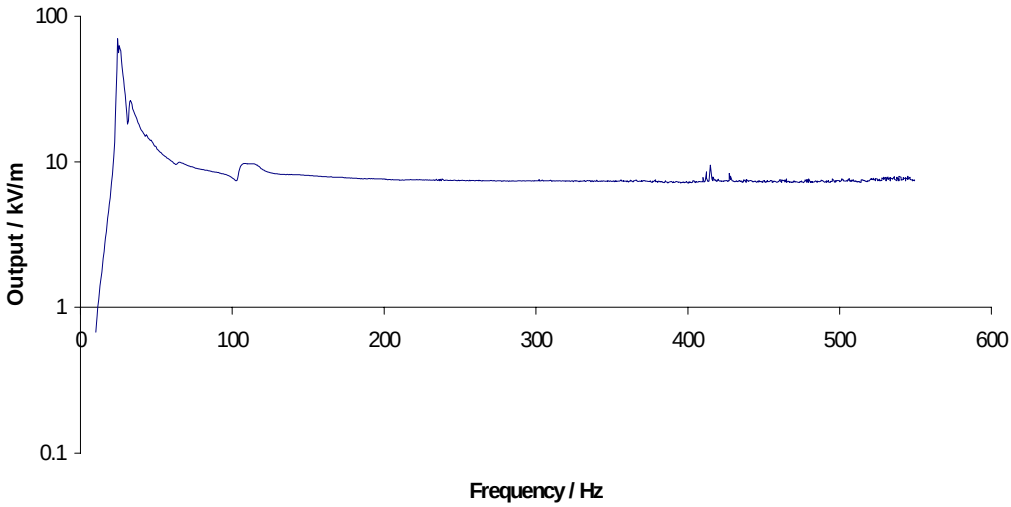

Figure 15 - Frequency response of a piezoelectric spring with a large seismic mass applied.

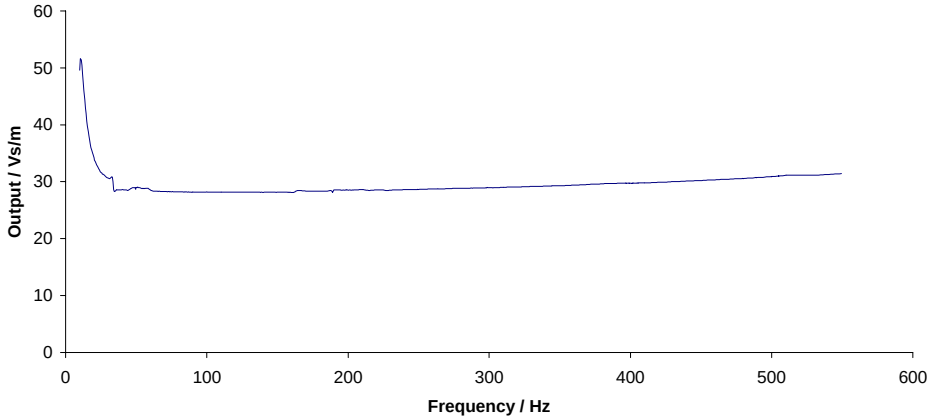

Figure 16 – Typical frequency response of a conventional geophone.

B.5. Conclusions and further work

Through many measured observations of the voltage output and frequency response of various geometries of piezoelectric springs, the main features of such devices have been recorded and understood. The results shown present a picture of how these springs behave in real vibration situations, which has uncovered many features of their operation. Piezoelectric springs behave in a completely different way to conventional geophones, and as such require different design rules. The effects of the self mass of a spring is one which demands the most attention, since it appears to be the dominant feature in causing the crowded frequency spectra observed to date. Methods to minimise this effect are, however, proposed, which do appear to point towards a more useable device in terms of response to vibrations over a wide frequency range.

Compared with the original ideas and aspirations, the work has progressed almost as expected. The complications of the frequency responses of the springs has made the work more difficult, but the predicted fundamental behaviour of the devices has been proven. Accurate measurements of distortion have yet to be taken on the devices, since the main problems have not yet been overcome, but the equipment obtained is capable of carrying out these measurements to an acceptable degree of precision.

The IRC now has a sophisticated and flexible system for measuring the response of devices to vibrations, and this will be useful in furthering this work to develop improved devices. Future work is planned on obtaining flatter frequency responses through the use of low stiffness springs of low mass, combined with relatively high seismic masses, while keeping the whole device as light as possible. The challenge to design a workable piezoelectric geophone is still great, but the results to date have shown promise for this approach. It is hoped that further interest in this work will allow this new technology to be taken much further. One potential use for a piezoelectric spring of the type worked with in this project has already been put forward, in the application of down hole well monitoring. In this case the piezo spring may be well suited, since it is proposed that the seismic mass is effectively the well itself, and therefore the response of a spring used will be much more predictable. Work on this application is continuing.

Appendix A - Spring Vibration Theoretical Considerations

A.1. - Units

E: Youngs Modulus	Pa
G: Shear Modulus	Pa
ρ: density	Kg m^{-3}
k_c: spring constant (compressive)	Nm^{-1}
k_R: spring constant rotational	Nm
k_f: spring constant (flexural)	Nm^{-1}
k_s: spring constant (shear)	Nm
d_0: outer diameter of tube	m
d_I: inner diameter of tube	m
D: major diameter of spring	m
n: number of active turns	
M: mass of the spring	Kg
m_0: effective mass of spring	Kg
m_s: applied seismic mass	Kg
J_A: second moment of area	m^4
J_P: polar moment of inertia	m^4
I_{R0}: moment of inertia of spring	Kgm^2
I_{Ra}: moment of inertia of seismic mass	Kgm^2

For a close-coiled helical spring, where the coils are in the form of a tubular section:

$$M = \frac{\pi D\left(d_0{}^2 - d_i{}^2\right)}{4}\rho$$

$$J_a = \frac{\pi\left(d_0{}^4 - d_i{}^4\right)}{64}$$

$$J_p = \frac{\pi\left(d_0{}^4 - d_i{}^4\right)}{32}$$

The required material constants for PZT-5A are the density (ρ = 7700 Kg m^{-3}), Young's modulus ($E=c^E_{11}$=110 MPa) and the shear or bulk modulus ($G=c^E_{66}$= 24.2 GPa).

A.2. - Compressive modes (longitudinal)

This is the usual mode in which a spring is employed, and consequently the most studied. A load is applied along the spring axis. A simple analytical model describes the deflection caused by such a load by considering the torque applied to the coils cross-section. The spring constant for a close coiled helical spring is given by the formula;

$$k_c = \frac{4\ J_p\ G}{\pi\ D^3 n}$$

Equation 2

The natural frequency (and higher resonances) can then be calculated for a spring where the ends are fixed:

$$f = \frac{1}{2}\sqrt{\frac{k}{M}} = \frac{2}{\pi\ D^2 n}\sqrt{\frac{G\ (d_0{}^2 + d_i{}^2)}{32\rho}}$$

Equation 3

For a spring with one end free to move, the resonant frequency occurs as though it were a spring twice the length whose ends are fixed. The resonant mode of a spring with a seismic mass is then the following:

$$f = \frac{1}{2\pi}\sqrt{\frac{k}{m_0 + m}}$$

Equation 4

Where m_0 is the effective mass of the spring, and m is the applied seismic mass. The effective mass of the spring, i.e. that proportion which contributes to the resonant frequency, works out at 0.4 of the total mass.

A.3. - Rotational Modes

A rotational mode is set up by a applying a torque to the spring in the plane of the coils, to coil or uncoil the spring. Such an action has also been extensively studied for helical torsion springs. The rotational spring constant k_R is given by;

$$k_R = \frac{E(d_0{}^4 - d_i{}^4)}{64\ D\ n}$$

Equation 5

The moment of inertia I_R of the spring about its own axis is simply

$$I_R = \frac{MD^2}{4}$$

Equation 6

A.4. - Shearing Modes

Shearing modes are the movement of the spring laterally, that is they are sheared between the base and the top. The spring constant for shearing k_S is given by;

$$k_S = \frac{8EJ_A}{\pi\ D^3}$$

Equation 7

The inertial term in the following calculations is assumed to be the mass of the spring

A.5. - Flexural Modes

Flexural modes occur from a bending moment applied in the plane of the spring axis. The spring constant for this mode therefore represents the moment required to twist the spring through one degree.

$$k_f = \frac{2E\ J_A}{\pi\ D\left(1 + \frac{E\,J_A}{G\,J_P}\right)}$$

Equation 8

For the resonance calculations of the flexural modes the inertial term is assumed to be the rotational inertia of a coil spinning about a diameter of the coil. In calculating this inertial term a simplification is made by assuming the diameter of the tube is small compared to that of the spring.
The following table presents simple equations for estimating the resonances of the piezoelectric spring, in all the spring constants used may be found in textbooks.

	Seismic mass	Both ends clamped
Compression	$f = \frac{1}{2\pi}\sqrt{\frac{k}{m_s}}$	$f = \frac{1}{2}\sqrt{\frac{k}{M}} = \frac{2}{\pi\ D^2 n}\sqrt{\frac{G\ (d_0{}^2 + d_i{}^2)}{32\rho}}$
Rotational	$f = \frac{1}{2\ \pi}\sqrt{\frac{E\left(d_0{}^4 - d_i{}^4\right)}{64\ D\ n\ I_s}}$	$f = \frac{1}{4D^2\pi\ n}\sqrt{\frac{E\left(d_0{}^2 + d_i{}^2\right)}{\rho}}$
Shearing	$f = \frac{1}{2\pi}\sqrt{\frac{E\left(d_0{}^4 - d_i{}^4\right)}{8D^3 m_s}}$	$f = \frac{1}{2D^2\pi\ n}\sqrt{\frac{E\left(d_0{}^2 + d_i{}^2\right)}{2\rho}}$
Flexural		$f = \frac{1}{2\,D^2\pi\ n}\sqrt{\frac{E\left(d_o{}^2 + d_i{}^2\right)}{\left(1 + \frac{E}{2G}\right)\rho}}$